Partitioning of reactive atmospheric nitrogen oxides at an elevated site in southern Quebec, Canada

K. L. Hayden and K. G. Anlauf
Meteorological Service of Canada, Environment Canada, Toronto, Ontario, Canada

D. R. Hastie
York University, Toronto, Ontario, Canada

J. W. Bottenheim
Meteorological Service of Canada, Environment Canada, Toronto, Ontario, Canada

Received 18 November 2002; revised 7 May 2003; accepted 28 May 2003; published 8 October 2003.

[1] Measurements of the major reactive nitrogen oxides including NO, NO_2, HNO_3, particulate nitrate, PAN, and NO_y, as well as O_3 and supporting meteorology, were made at an elevated site (845 masl) in the rural eastern townships of Quebec, Canada, from February 1998 to October 1999. NO_x (and NO_y) mixing ratios exhibited a distinct seasonal cycle with median NO_x levels in winter more than a factor of 4 greater than in summer. Seasonal partitioning indicated that NO_x was the dominant fraction of NO_y during winter (>70%), with HNO_3 and PAN fractions of <18 and 9%, respectively. The NO_y reservoir in summer consisted of average contributions from NO_x, HNO_3, and PAN of 35, 20–25, and 13%, respectively. A NO_y deficit of the order of 25–30% was observed during spring and summer that could not be explained by measurement uncertainties or potential interferences. It is possible that there were other reactive nitrogen species in the atmosphere that were not separately measured that contributed to the NO_y deficit. Indications are that these compounds were photochemically produced and present in highly processed air masses. *INDEX TERMS:* 0345 Atmospheric Composition and Structure: Pollution—urban and regional (0305); 0365 Atmospheric Composition and Structure: Troposphere—composition and chemistry; 0368 Atmospheric Composition and Structure: Troposphere—constituent transport and chemistry; *KEYWORDS:* nitrogen oxides, partitioning, rural

Citation: Hayden, K. L., K. G. Anlauf, D. R. Hastie, and J. W. Bottenheim, Partitioning of reactive atmospheric nitrogen oxides at an elevated site in southern Quebec, Canada, *J. Geophys. Res.*, *108*(D19), 4603, doi:10.1029/2002JD003188, 2003.

1. Introduction

[2] An understanding of the processes that govern the formation, distribution and removal of the reactive nitrogen oxides is necessary in order to elucidate their relative importance in the tropospheric oxidation chemistry cycle. Ambient levels of NO_x ($NO + NO_2$) play an important role in the formation and destruction of tropospheric O_3. Anthropogenic and biogenic sources of NO_x are highly variable and atmospheric mixing ratios exhibit a large dynamic range. In rural environments, where NO_x levels can be less than a few ppbv, O_3 production is limited by the available NO_x, and modeling studies suggest that this dependence is nonlinear [*Liu et al.*, 1987]. Removal of NO_x from the atmosphere is primarily through oxidation to form HNO_3 with subsequent loss through wet and dry deposition. Other reactions can also result in the formation of organic nitrates, HONO, NO_3, HO_2NO_2 and particulate nitrate. These products can act as either temporary NO_x reservoirs or sinks. The formation and removal processes of these oxidized products of NO_x are complex with a non-uniform distribution both spatially and temporally. In order to understand these processes, it is essential to quantify these species, particularly in relation to the total odd nitrogen (NO_y). Total odd nitrogen, (NO_y) is defined as the sum of all the gaseous inorganic nitrogen oxides: $NO + NO_2 + HNO_3 + PAN + HONO + HO_2NO_2 + NO_3 + 2N_2O_5$ + other organic nitrogen-containing compounds. It has been recognized that biogenic hydrocarbon emissions can play a significant role in O_3 formation [*Trainer et al.*, 1987, 1993]. Concurrent measurements of reactive nitrogen oxide species, O_3, hydrocarbons and meteorology in forested areas are thus important to determine the significance of biogenic emissions in the tropospheric photochemical cycle of such environments.

[3] Measurements of O_3 and meteorological parameters have been made since late 1986 at the elevated research site (845 masl) in Sutton, Quebec. The site is located in the rural eastern townships just north of the Quebec-Vermont border and is largely surrounded by mixed forest. One of the main research goals for these measurements is to determine the long-term seasonal trends in background O_3 levels. From

0148-0227/03/2002JD003188$09.00

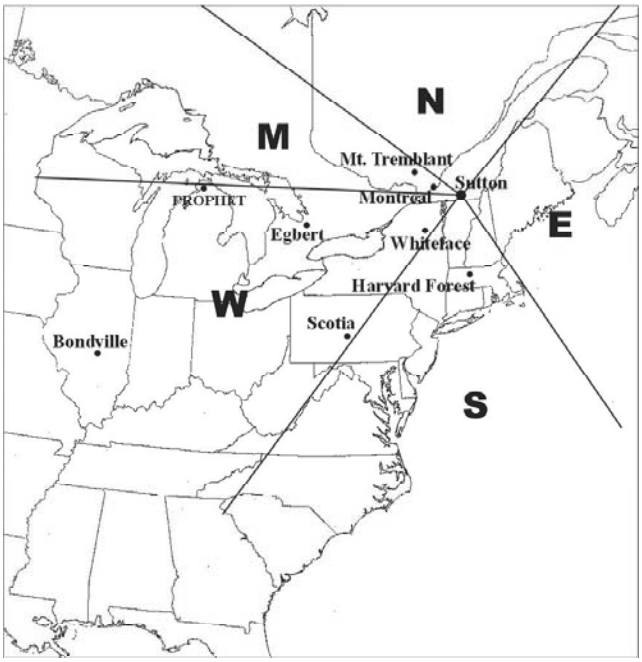

Figure 1. Map of northeastern North America showing the location of the Sutton sampling site, as well as other locations noted in the text. Also shown are the air mass sectors as defined by the locally measured wind direction.

February 1998 to October 1999, detailed measurements were made of the major reactive nitrogen oxides including nitric oxide (NO), nitrogen dioxide (NO_2), nitric acid (HNO_3), particulate nitrate (p-NO_3^-), peroxy acetyl nitrate (PAN) and NO_y. The measurement of NO_y represents the signal derived from the Mo converter channel of the TECO 42S nitrogen oxides analyzer where reactive nitrogen oxides are converted to NO for detection. In addition, for approximately two weeks in the summer of 1998 (July 13–29) and 1999 (June 27–July 15), more intensive measurements were made, primarily to obtain higher time-resolved HNO_3 data. To our knowledge, no such other long term data sets with coincident measurements of the significant reactive nitrogen oxides, as well as O_3 and the supporting meteorology, exist anywhere in Canada.

[4] The main objective of this particular study was to determine the seasonal variations in the concentrations and the partitioning of the major reactive nitrogen oxides at Sutton. An emphasis was on how these species varied as a function of air mass origin, and their behavior in air masses with different degrees of photochemical processing.

2. Experimental

[5] The Sutton research site (45°05′19″N, 72°33′25″W) is located at the top of a ski hill (845 masl) in the eastern townships of the province of Quebec. Figure 1 is a map of northeastern North America showing the location of the town of Sutton, approximately 7 km north of the Vermont-Quebec border. Sutton is in a rural, hilly area and the measurement site is surrounded by mainly a mix of deciduous and coniferous trees with grass-covered open clearings. The largest urban center, Montreal, is located 90 km northwest of the site (pop: 3 438 500 July 1, 1999, Statistics Canada). The St. Lawrence Lowlands (large-scale agricultural areas and small urban centers) are 50 km to the north and beyond, and in the south-southwest quadrants are the Appalachians with no large communities or agricultural areas for several hundred km. The sampling hut is located on a slight knoll above the surrounding terrain of the ski hill and was thermostatically controlled for temperature by electric heaters and air conditioners. The filtered inlets to the gas analyzers were mounted on a railing on the roof of the hut about 5 m above the ground. Meteorological instrumentation was mounted on a tower on the roof of the hut. The filter pack system was on a separate tower on the roof, putting the filter packs at 7 m above the ground.

2.1. NO and NO_2

[6] Ambient air was sampled through 0.65 cm OD PFA Teflon tubing of approximately 4 m in length. Alternating 1 min measurements of NO and NO_2 were made using an Ecophysics model CLD770 NO analyzer (based on the chemiluminescence of the NO + O_3 reaction); an Ecophysics model PLC760 photolytically converted a fraction of ambient NO_2 to NO using a 300W high-pressure Xenon arc lamp that was filtered to 320–420 nm for high NO_2 selectivity. The background signal was determined for each channel (either NO or NO_2 pathway) every 10 minutes by reacting ambient air with excess O_3 in a pre-chamber and then measuring this signal in the main reaction chamber. Calibrations were done once per day by switching from ambient sampling mode to sample calibration gas. An automated Environics Series 100 dilution system prepared calibration gas by mixing dried zero air made with an AADCO zero air generator (model 737–10) and NIST-referenced NO cylinder gas (NO in N_2, SRM 2628a, 9.67 ± 0.15 ppm). The efficiency of the photolysis conversion was also monitored daily using NO_2 produced from incomplete gas phase titration of the NO standard with O_3. Typically, NO levels were near 70 ppbv and O_3 was approximately 25 ppbv. The detector sensitivity to NO of a first instrument setup decreased from 429 to 347 cps $ppbv^{-1}$ over a period of 244 days, and a second replacement instrument system drifted from 650 to 550 cps $ppbv^{-1}$ in 297 days. The Xenon lamp was replaced 3 times during the campaign and typically decreased in efficiency from 80 to 40% in less than 200 days. The lamps were replaced when the efficiency dropped to 40–50%. At the 3σ level for a one-minute integration time, the detection limit was determined to be 30 pptv for NO and 60 pptv for NO_2. At night, when NO was completely titrated by O_3 (excess O_3 at night), the measurement signal could not be distinguished from the background signal within the detection limits.

[7] Since the calibrations were done using dry air, laboratory tests were conducted to compare the detector sensitivity to NO in humidified versus dry air. It was determined that the ratio of the humidified signal to the dry signal (R), varied linearly with absolute humidity (AH, expressed as parts per thousand by volume (ppthv)): $R = -0.00265 \times (AH) + 0.990$). Figure 2 shows a plot of this humidity dependence. Individual NO and NO_2 mixing ratios were corrected for the water vapor influence using the ambient measurements of relative humidity, pressure and air temperature to calculate the absolute humidity. The mean

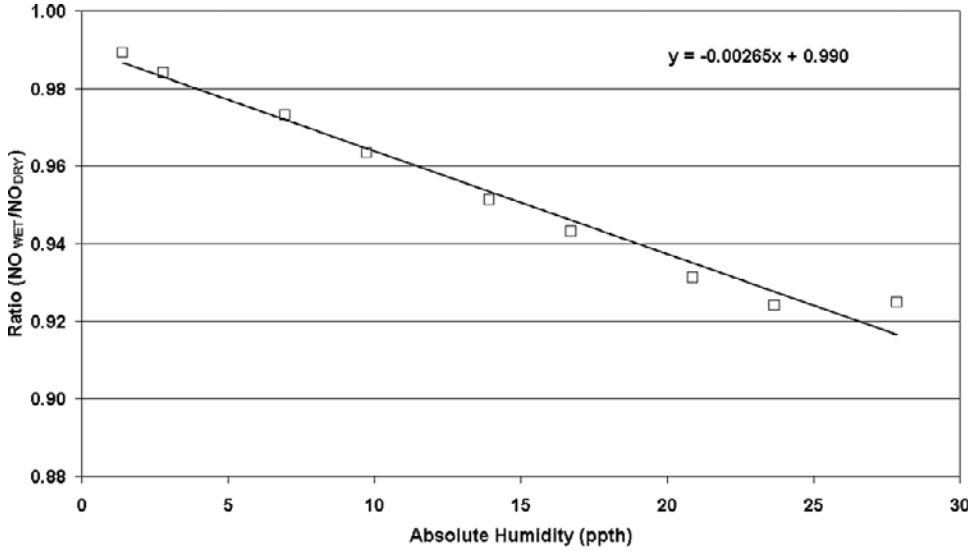

Figure 2. Ratio of the humidified signal to the dry signal as a function of absolute humidity as determined using the Ecophysics NO/NO_2 instrumentation.

absolute humidity ranged from 15.7 ppthv in summer (78% RH, 16°C) to 4.09 ppthv in winter (85% RH, −6.8°C), corresponding to average correction factors, R, of 0.948 and 0.980 respectively.

[8] Also, 1-min NO and NO_2 mixing ratios were corrected for interference from ambient O_3 reactions along the inlet tubing and within the photolysis cell [*Ridley et al.*, 1988; *Fehsenfeld et al.*, 1990; *Bollinger*, 1982]. With a residence time of 4 s in the photolysis cell and 2 s through the inlet, only small interferences were calculated and NO mixing ratios were altered by about 3% and NO_2 values by 1%.

[9] NO and NO_2 data were quality assured by removing any erroneous data due to instrument malfunctions, data collection errors and known instrument contamination from local sources. Less than 2% of the data was excluded. The background signal was subtracted from the raw 1-min photon count rates using the closest value in time to a particular measurement. Mixing ratios of NO and NO_2 were calculated by applying interpolated sensitivity factors and interpolated NO_2 conversion efficiencies. Since the NO_2 channel is the sum measure of NO plus a fraction of converted NO_2, mixing ratios of NO_2 were calculated by subtracting interpolated NO mixing ratios.

[10] The uncertainty of the NO/NO_2 measurements in terms of calibration uncertainties is dependent upon the cylinder calibration accuracy, uncertainty in the flow controller calibrations, variations in the individual calibrations, variations in calibration points, the uncertainty in the background signal, the NO_2 conversion efficiency uncertainty, and the NO_2 calculation uncertainty (accuracy of the interpolated NO value). Flow controllers were calibrated before and after the field campaign, and their combined estimated uncertainty was less than 1%. The standards on the NO_y, NO/NO_2 and PAN measurement systems were all referenced to one primary NO standard that came directly from the National Institute for Standards and Technology (NIST). This NIST cylinder was also cross-checked with two other NIST cylinders of different ages that indicated its concentration had remained stable. The NO calibration standards were accurate to within 3.5%. After including the variations in the calibration points (<5%) and an estimate of the uncertainty in the background signal (8%), the total uncertainty propagated through the individual uncertainties was determined to be less than ±(16% + 30 pptv) for NO and ±(21% + 60 pptv) for NO_2 (3σ, 1-min).

2.2. NO_y

[11] A Thermo Environmental Instruments Incorporated (TEII) Model 42S instrument was used to make 3-min measurements of NO_y species (and NO). Oxides of nitrogen were reduced to NO by passing the ambient air over molybdenum heated to 325°C. The entire converter unit was housed on the roof of the sampling hut (5 m above ground) and as close as possible to the inlet to minimize sample loss prior to conversion. The length of the PFA Teflon inlet from the filter to the converter was about 20 cm and was not heated (the Teflon inlet tube extended well into the converter inlet). At the ambient inlet a Teflon filter removed particulates from the ambient air so that the NO_y measurement would not include a signal from particulate nitrate. This filter was changed once per week by the local operator during normal operation, and, once per day during the intensive measurement periods. The background signal was determined by reacting ambient air with excess O_3 in a pre-chamber and then measuring this signal in the main reaction chamber. An internal microprocessor automatically corrected the sample measurement for the pre-chamber background resulting in only a net analog signal output. NO_y measurements were alternated with those of NO by switching ambient air to bypass the converter. The calibration system, which was completely separate from the Ecophysics NO/NO_2 setup, consisted of an Environics Series 100 calibrator that mixed flows from a NIST-referenced NO gas transfer standard and zero air that was produced by filtering room air through charcoal, drier cartridges and a molecular sieve. The calibration gas was introduced once per day immediately after the Teflon inlet

filter with excess venting out the inlet. The instrument sensitivity to NO was expressed as ppb mV^{-1}. The efficiency of NO_2 conversion was also monitored during these daily calibration routines by means of gas phase titration reaction of a NO standard with O_3. The efficiency of NO_2 conversion was 100% within measurement uncertainty. Conversion efficiencies for other NO_y species like HNO_3 and PAN were not evaluated during this field campaign. The ambient NO mixing ratios determined from the Ecophysics instrument and the TECO NO_y system differed by less than 5% providing confidence in the integrity of the separate calibration systems. At the 3σ level for a three-minute averaging period, the detection limit was determined to be 90 pptv.

[12] As with the Ecophysics NO/NO_2 system, laboratory tests were conducted to compare the detector sensitivity to NO in humidified versus dry air. The ratio of the humidified signal to the dry signal (R), varied linearly with absolute humidity (AH, expressed as parts per thousand by volume (ppthv)): $R = -0.0029 \times (AH) + 0.996$). Individual NO and NO_y mixing ratios were corrected for the water vapor influence using the ambient measurements of relative humidity, pressure and air temperature to calculate the absolute humidity. The mean absolute humidity ranged from 15.7 ppthv in summer (78% RH, 16°C) to 4.09 ppthv in winter (85% RH, −6.8°C), corresponding to average correction factors, R, of 0.951 and 0.984 respectively.

[13] NO_y was quality assured by removing any erroneous data due to instrument malfunctions, data collection errors and known instrument contamination from local sources. Less than 1% of the data was excluded. 3-min NO_y mixing ratios were calculated by applying interpolated sensitivity factors to the zero-corrected voltages.

[14] The uncertainty in the NO_y measurement is dependent on the same factors as for the Ecophysics NO/NO_2 system (except NO interpolation uncertainty). The uncertainty of NO_y due to known factors was estimated to be ±(11% + 90 pptv) (3σ, 3-min). This uncertainty is smaller than for the Ecophysics NO/NO_2 measurements mainly because the zero is determined more frequently. It is recognized that some HNO_3, PAN and other NO_y species may be lost through the inlet or not converted efficiently to NO, however, we assume the conversion efficiencies for HNO_3 and PAN to be 100% to provide a lower limit on NO_y. Potential interferences in the NO_y measurement referred to in the literature are discussed in terms of an NO_y deficit in section 3.6.2.

2.3. PAN

[15] PAN was measured every 30 minutes using a modified Shimadzu Mini2 gas chromatograph with an electron capture detector held constant at 850 torr. Ambient air was drawn in at 200 ml min^{-1} through a Teflon filter and a 1/8″ Teflon line to a 10 cm^3 conditioned stainless steel sampling loop. Separation was achieved isothermally (40°C) on a 50 cm long, 6.3 mm outer diameter silanized Pyrex glass column filled with 5% Carbowax-400 on Chromosorb G-AW (DMCS, 100–120 mesh) and using ultrahigh-purity nitrogen as a carrier gas. Calibrations were performed every few months with a Meteorologie Consult GmbH calibrator which is based on the photolysis of a mixture of acetone and a known quantity of NO to produce PAN. Integrated PAN peak areas were converted to mixing ratios using an average calibration factor for the measurement campaign. The calibrations varied by about 7%. These calibrators have been extensively tested by *Pätz et al.* [2002] and found to convert NO into PAN with a 90% ± 5% efficiency, and for these calibration calculations a factor of 0.9 has been incorporated. PAN measurements were estimated to be accurate to within 15–20% with uncertainties related to the average calibration factor used, peak area integration, flow controller and cylinder calibrations and conversion efficiency of acetone to PAN in the calibrator.

2.4. HNO_3 and p-NO_3^-

[16] Gaseous HNO_3 and particulate NO_3^- were measured using a triple-stage filter pack sampling system. Ambient air was sampled at approximately 25–30 LPM through three different filters mounted in a triple-stage filter pack: a 47 mm, 1μm pore size Teflon front filter to trap particulates; a 47 mm 1μm pore size nylon middle filter to remove gaseous HNO_3, and a final Whatman 41 filter impregnated with an aqueous solution of K_2CO_3/glycerol to collect gaseous SO_2 [*Anlauf et al.*, 1986]. Field blanks were obtained by mounting a prepared filter pack in the same manner as the filter packs being sampled, but ambient air flow was excluded. The sampled filters were extracted and analyzed by ion chromatography by the Canadian Air and Precipitation Monitoring Network (CAPMoN) laboratory at the Meteorological Service of Canada in Toronto, Ontario. During normal operation, daily samples between 1000 and 1600 EST were collected, and during two summer intensive measurement periods, filter samples were taken at a higher time resolution of every 2 to 4 hours around the clock for approximately 2 weeks in duration. HNO_3 and p-NO_3^- uncertainties were determined from uncertainties in flow meter calibrations, laboratory analysis, and blank variations (largest uncertainty). A blank uncertainty of 6.1% for HNO_3 and 19% for particulate nitrate was based on 2σ above the mean blank level. More than 95% of the HNO_3 and 81% of the particulate nitrate measurements in 1998 and 1999 were above the 2σ blank level. The few mixing ratios less than this were close to the detection limit and have very large uncertainties; these values were excluded. The total propagated uncertainty was determined to be 10% for HNO_3 and 24% for particulate nitrate. These uncertainties represent lower limits because they do not account for potential interferences in the measurement technique and there was no HNO_3 calibration. The main interference discussed in the literature is from evaporation of ammonium nitrate particles on the front Teflon filter with a corresponding increase in HNO_3 on the nylon middle filter [*Forrest et al.*, 1982; *Spicer et al.*, 1982; *Fehsenfeld et al.*, 1998]. There is also the possibility of HNO_3 loss on particles trapped on the front Teflon filter. These artifacts are potentially important with high-aerosol loadings, high temperatures and low relative humidity. It is expected that such interferences would be minimal at Sutton because, for example, in summer, aerosol loadings are low (mean 4.4 ug m^{-3}), temperatures are moderate (mean 19°C) and the mean relative humidity is 69%. Furthermore, an intercomparison study in North Carolina indicated close agreement between the filter pack and the tunable diode laser technique, and the

Table 1. Statistical Summary of the Daytime Hourly Mixing Ratios of NO, NO_2, NO_x, NO_y, PAN, and O_3, and the Integrated Daytime Mixing Ratios of HNO_3 and p-NO_3^- Grouped by Season[a]

Season	Statistic	NO_x	NO_y	PAN	HNO_3	p-NO_3^-	O_3
Winter, DJF	Mean	2.39	3.11	0.18	0.35	0.44	35.11
	Median	1.49	2.33	0.15	0.20	0.28	35.69
	Upper 67‰	4.25	5.13	0.27	0.68	0.78	43.08
	Lower 67‰	0.63	1.05	BDL	BDL	BDL	26.72
	N	319	694	319	57	57	319
Spring, MAM	Mean	1.10	2.50	0.33	0.47	0.25	35.11
	Median	0.62	2.03	0.27	0.30	0.19	46.17
	Upper 67‰	1.59	3.61	0.48	0.78	0.30	56.04
	Lower 67‰	0.34	1.26	0.17	0.09	0.05	38.33
	N	765	1006	765	128	128	765
Summer, JJA	Mean	0.47	1.82	0.28	0.54	0.15	41.57
	Median	0.37	1.64	0.23	0.35	0.12	38.71
	Upper 67‰	0.62	2.65	0.43	0.86	0.25	54.66
	Lower 67‰	0.26	1.02	0.12	0.16	BDL	28.29
	N	689	649	689	156	156	689
Fall, SON	Mean	1.63	2.34	0.22	0.28	0.19	28.53
	Median	1.05	1.97	0.12	0.17	0.11	29.36
	Upper 67‰	3.05	3.16	0.36	0.47	0.25	32.29
	Lower 67‰	0.52	1.13	BDL	BDL	BDL	19.99
	N	186	186	186	31	31	186

[a]Mixing ratios are in ppbv. Daytime hourly, 1000–1600 EST; daily integrated, 1000–1600 EST; DJF, December, January, February; MAM, March, April, May; JJA, June, July, August; SON, September, October, November; BDL, below detection limit.

duration of filter pack sampling times did not affect the measured HNO_3 concentration [*Anlauf et al.*, 1987].

2.5. O_3 and Meteorology

[17] O_3 was measured with a commercial TECO Model 49 instrument based on the principle of ultraviolet absorption by O_3. Calibrations were performed approximately every 3–4 months and were referenced directly to the National Institute for Standards and Technology (NIST). Meteorological measurements were made of temperature and relative humidity (CSI model HMP45CF), pressure (CSI model Met-One 090B), total ultraviolet radiation (295–385 nm) (Eppley model TUVR), total spectrum solar radiation (LiCOR Model LI-200SZ), precipitation (Sierra model 2501 tipping bucket rain gage), wind speed (Met-One model 013A) and wind direction (Met-One model 023A).

2.6. Data Averaging

[18] Data recovery for NO_x ($NO + NO_2$) and NO_y was approximately 60% and 67% respectively. Interruptions in operation were mainly due to power failures that led to instrument malfunctions. No NO_y measurements were recoverable from July 14–November 5, 1998 because of a failed photomultiplier tube, but measurements were continued until November of the following year for better data capture of the summer and fall seasons. An instrument problem resulted in discontinued NO_x measurements in early September 1999. PAN measurements were available for 90% of the field campaign and HNO_3 was recovered for 97% of the period. 98% of the O_3 measurements were available.

[19] Two databases were created: (1) an hourly-averaged database that included NO, NO_2, NO_y, O_3, PAN and meteorological parameters, and (2) a database with NO, NO_2, PAN, NO_y, and O_3 averaged over the HNO_3/particulate nitrate sampling intervals (daily 1000–1600 EST in normal operation and 2–4 hour intervals during the summer intensives). The highest time resolved measurements for each species were used to calculate these averages only if more than 75% of the data was available in a particular averaging period. Since the PAN measurements represent essentially instantaneous samples every 30 minutes, time-weighted hourly averages were calculated in order to best represent PAN mixing ratios for a particular hour. The averages in these databases were carefully checked to ensure that they were the best possible values for the interval. In database (2), for each HNO_3/particulate nitrate sampling interval, the constituent NO_y species were summed to derive $\sum NO_{yi}$ and then ratios and differences were calculated using the measured NO_y. Also, ratios of the individually measured nitrogen oxide species with NO_y were calculated.

3. Results and Discussion

3.1. Observations

[20] Table 1 is a statistical seasonal summary of the daytime (1000–1600 EST) hourly mixing ratios of NO, NO_2, NO_x, NO_y, PAN and O_3, and the daily integrated samples (1000–1600 EST) of HNO_3 and p-NO_3^-. The statistics in this table are based on daytime data collected over the entire measurement period and are coincident with each other (except for NO_y because of the large data gap in the summer/fall 1998). Since the campaign ran from February 1998 to October 1999, the seasons are not equally distributed with respect to data capture.

[21] NO_x and NO_y exhibited a distinct seasonal cycle with levels in winter higher than in summer. For example, the median NO_x mixing ratio was more than a factor of 4 greater in winter compared to summer. Also, the range of NO_x and NO_y mixing ratios in winter was greater than in summer. The influence of a number of high-NO_x excursions in winter can be seen in differences between the mean and median. Monthly median mixing ratios of NO_x oxidation products, including PAN and HNO_3, were higher in the spring and summer months compared to the winter and fall seasons. In addition, the central range of HNO_3 and PAN values indicated higher levels during summer compared to winter. Mixing ratios of p-NO_3^- were low overall, with levels slightly higher in winter and spring compared to summer. The median O_3 mixing ratio was highest in spring and lowest in fall.

[22] The seasonal differences in NO_x levels cannot be explained by variations in NO_x emissions because the source strength of NO_x appears to be independent of season [E. Voldner et al., $1^\circ \times 1^\circ$ global SO_x and NO_x 2-level inventory resolved seasonally into emission sectors and point and area emission sources, available at www.ortech.ca/cgeic/poster.html, 1997; *Meteorological Service of Canada*, 2001]. It is thus important to consider both the effects of the boundary layer, particularly since Sutton is an elevated site, deposition and photochemistry. Using the CALMET meteorological model that incorporates vertical temperature and wind data, as well as surface-based meteorological measurements, *SENES Consultants Ltd.* [1997] calculated hourly mixing heights for North America. These results indicate a moderate seasonal variation in afternoon

mixing heights at the Sutton location (e.g., winter-1200 m; summer -1450 m). The small variation in mixing heights would only marginally affect the seasonal differences in nitrogen oxide levels. The much earlier results of *Holzworth* [1967] showed greater seasonal differences in mixing heights, but this work was based on rough approximations and assumptions. It is also apparent that these mixing heights put the Sutton site well within the mixed boundary layer (cf. elevation of Sutton site above valley floor is about 600 m). Mixing within the boundary layer has also been inferred through seasonal O_3 measurements made at the elevated Sutton site compared with those from a valley site (Sutton Valley, 250 masl) located about 10 km from the base of the mountain [*NO_x/VO_c Science Assessment*, 1997]. In this analysis it was shown that in all seasons there was little diurnal variation in O_3 mixing ratios at the Sutton elevated site (also depicted in Figure 3), but the valley site showed a strong diurnal variation typical of valley or flat-land sites (strongly influenced by nocturnal surface-based inversions). However, by midday (1100–1600 EST), O_3 levels at the Sutton Valley site closely matched those at Sutton Ridge indicating that the boundary layer had been fully developed and mixed. Thus the daytime chemical mixing ratios observed at the Sutton mountain site are considered to be representative of the boundary layer. Since seasonal boundary layer height differences do not appear to be a significant factor contributing to seasonal NO_x differences, it follows that photochemistry must play a dominant role in determining the seasonal nitrogen oxide levels. One would expect that summertime photochemistry would enhance NO_x oxidation leading to lower NO_x levels in summer, and increase oxidized products like HNO_3 and PAN. The increased importance of these oxidized species in summer is apparent from the measurements which showed higher levels compared to the winter. This is also consistent with the results of *Munger et al.* [1996, 1998] who found that the overall chemical lifetime of NO_x due to oxidation and deposition increased from a minimum of 0.3 days in summer to 1.5 days in winter, and the lifetime of NO_y ranged from 1 day in summer to more than 2 days in winter months.

[23] The seasonal diurnal variations of all of the hourly measured nitrogen oxide compounds, ozone and radiation measured at this elevated site are shown in Figure 3. In all four seasons, NO mixing ratios had a broad daytime maximum that coincided with the radiation measurements, reflecting NO_2 photolysis. Largest NO levels occurred during winter, partly because NO_2 was higher during this season, and also because of a higher albedo in winter resulting in increased actinic flux. In winter, NO_2, much like NO_y, showed a steady increase throughout the day to maximize at night, whereas, in fall, NO_2 had a shallow minimum during the day. In summer, a broad minimum during the day was observed in NO_2 and then maximized at night, but, in spring, NO_2 levels were higher and more constant. In summer, NO_y mixing ratios were remarkably constant near 1.5 ppbv, whereas more diurnal variability was observed in the other three seasons. As previously noted, little diurnal variation was observed in O_3 mixing ratios in all seasons. This behaviour is consistent with other high elevation O_3 measurements that are minimally influenced by nocturnal inversions [*Aneja et al.*, 1994]. Sectoring the data by air mass origin revealed that the slight spring/summer diurnal variation in PAN and O_3 as seen in Figure 3 is mainly due to the N and M sectors, whereas, the S and W sectors showed insignificant variation. However, in the winter season, all nitrogen oxides exhibited substantial and differing variability among sectors; the fall period was similar to winter, but not as definitive because of the limited database. It should be noted that the winter diurnal NO_x profile represents a composite of a number of episodes that were variable as to time of day, duration and magnitude. This variability is consistent with wintertime meteorology being more favorable to faster transport, stronger surface inversions and a more heterogeneous boundary layer structure. Further analysis of these individual episodes are required to clarify the effect of these contributing factors on NO_x at Sutton.

3.2. Comparison to Other Measurements

[24] It is instructive to have a composite picture of the range of nitrogen oxide mixing ratios at rural locations in eastern North America (refer to Figure 1 for site locations). In Figure 4a, seasonal measurements of NO_x, NO_y and NO_x/NO_y at Sutton (SU) are shown together with those at Harvard Forest (HF) (1990–1993), a rural site in Petersham, Massachusetts. SU and HF showed comparable seasonal NO_x and NO_y cycles with a winter maximum and a summer minimum see Figure 4a(i) [*Munger et al.*, 1996] (percentiles obtained from *Emmons et al.* [1997]). However, the measured range of NO_x and NO_y mixing ratios were consistently lower at SU in all seasons. The NO_x/NO_y ratios at SU also exhibited a similar seasonal pattern as HF with higher ratios in winter compared to summer. This is expected to be largely due to enhanced conversion of NO_x to oxidized species like HNO_3 and PAN in the summer.

[25] Figure 4b compares the Sutton data to measurements made during summer at several rural sites (percentiles for Kinterbush, Bondville, Scotia, HF, and Egbert in Figure 4b are from *Carroll and Thompson* [1995]). For example, during a 4-week field campaign in the summer of 1988, NO_x mixing ratios at several locations (Bondville IL, Egbert ON, Scotia PA, Whiteface NY, Whitetop VA, Brasstown Bald GA) ranged by more than an order of magnitude indicating substantial influence from anthropogenic emissions [*Parrish et al.*, 1993]. Also, NO_x levels were higher by more than a factor of 2 compared to Sutton. In fact, the median values at Sutton do not even fall within the central two-thirds of the mixing ratios measured at most of these sites. It is evident from Figure 4b that NO_x levels and NO_x/NO_y ratios at SU are most comparable to those at HF and the PROPHET site, all less impacted by anthropogenic emissions.

3.3. Air Mass Origin

[26] Identification of the origin of air masses can provide information on the atmospheric processes that contribute to the observed chemical concentrations. It was speculated that there would be occasional anthropogenic influence on the site, particularly related to emissions from Montreal, a major urban center 90 km to the northwest. In order to segregate Montreal air from 'cleaner' more northerly air and to separate sources from the south and the west, five sectors were defined using the locally measured wind direction (depicted in Figure 1): a northerly sector N (334°–44°) that

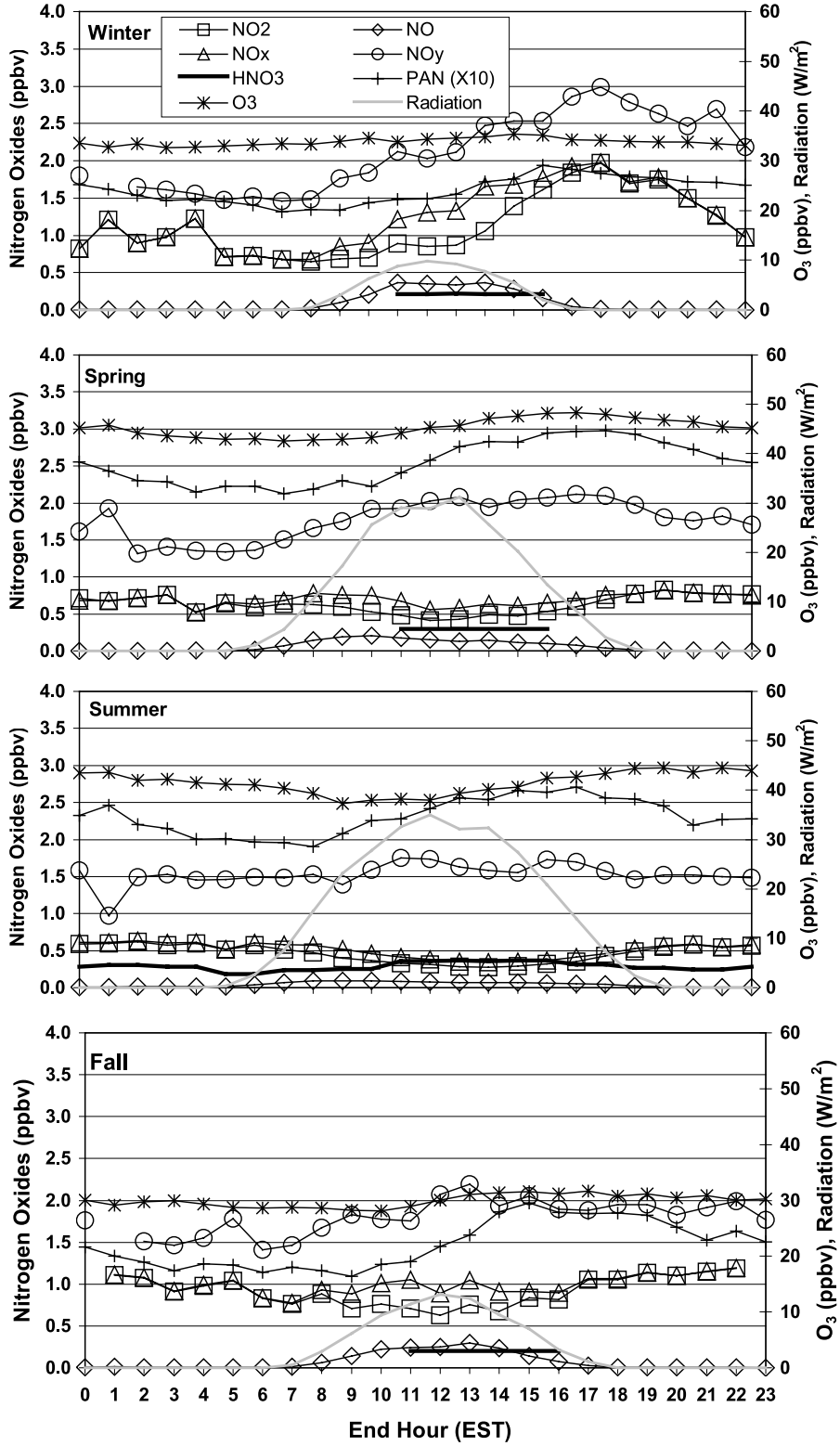

Figure 3. Diurnal variation of the measured nitrogen oxide species, ozone, and radiation for all hourly data (with the exception of the integrated HNO_3 samples) in each season. The points represent the median ending hourly value.

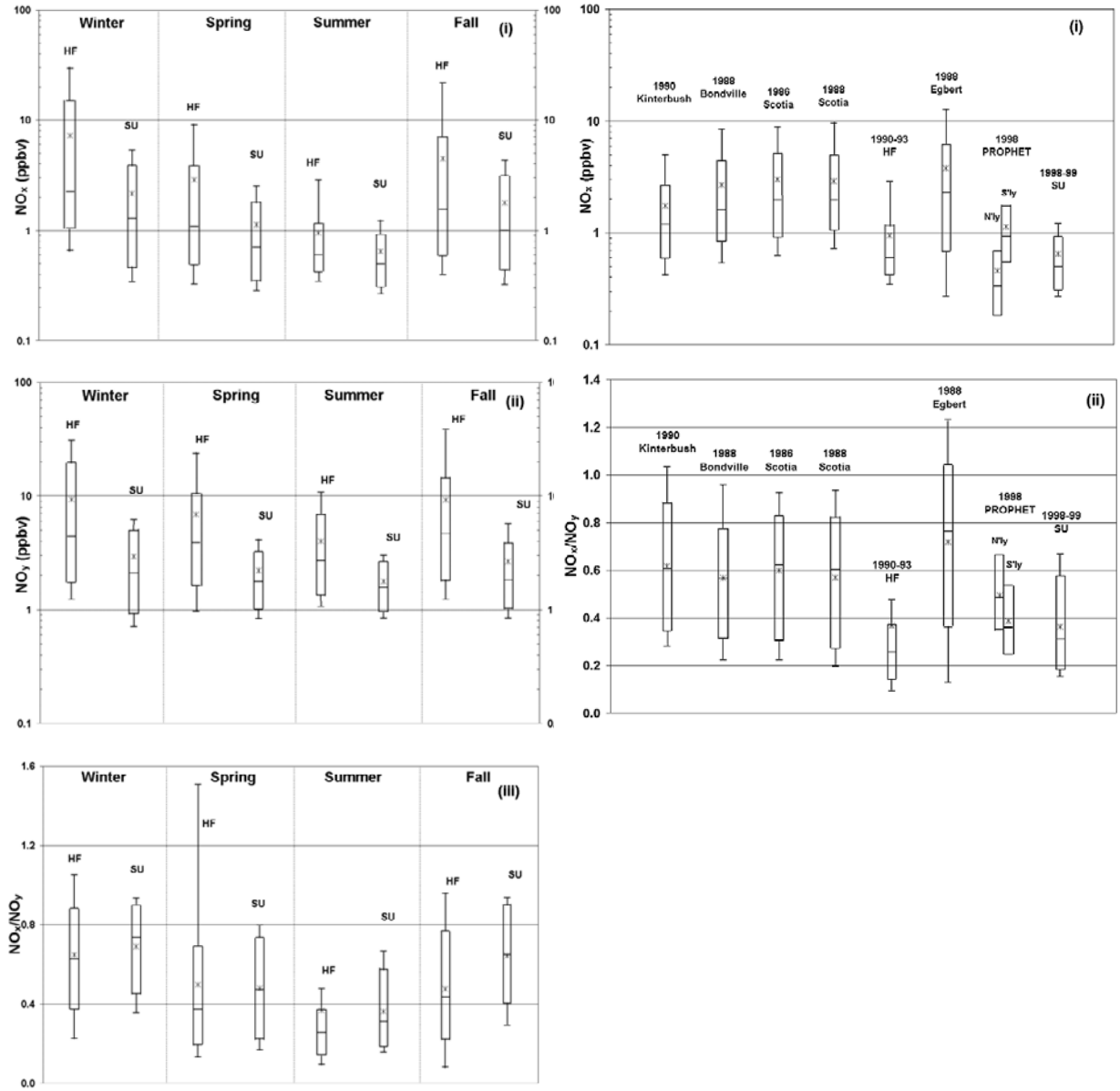

Figure 4. (a) The seasonal distribution of (i) NO_x, (ii) NO_y, and (iii) NO_x/NO_y at Harvard Forest, MA (HF) and Sutton, Quebec (SU). Each box encompasses 67% of the central portion of data, and the vertical lines extend to include 90% of the measurements. The median is shown as a horizontal line within the box and the mean is indicated with a star symbol. Refer to Figure 1 for a map showing the location of HF. The Sutton data are based on all of the hourly measurements. (b) The distribution of (i) NO_x and (ii) NO_x/NO_y in summer at selected continental, rural sites in North America, including Sutton, Quebec. Figure details are same as in Figure 4a. N'ly, northerly flow; S'ly, southerly flow.

was directly north of the site in a region with no major emission sources, a north westerly sector, M, that included the city of Montreal (278°–334°), a westerly sector W (220°–278°) that excluded Montreal, but encompassed sources along the westerly section of the region known as the Windsor-Quebec corridor, a southerly sector S (156°–220°) across the Canada-United States border with major emission sources being the cities of Boston, New York and Philadelphia, and an easterly sector E (44°–156) that was primarily marine-influenced. An analysis of the air mass origin using back trajectories related to the measurements in this study has not yet been carried out. However, previous work has been done to compare the locally measured wind direction (at wind speeds >2 m s^{-1}) with isobaric five-day back trajectories from Mt. Sutton at 925 mb calculated with the Environment Canada trajectory model [*Olson et al.*, 1978]. In this comparison, 9 years of trajectories were visually classified into defined sectors if they remained within the same sector for at least 3 days. Each trajectory was related to the measured O_3 at the site and average O_3 mixing ratios were calculated for each sector. These mixing ratios were then compared with those obtained from

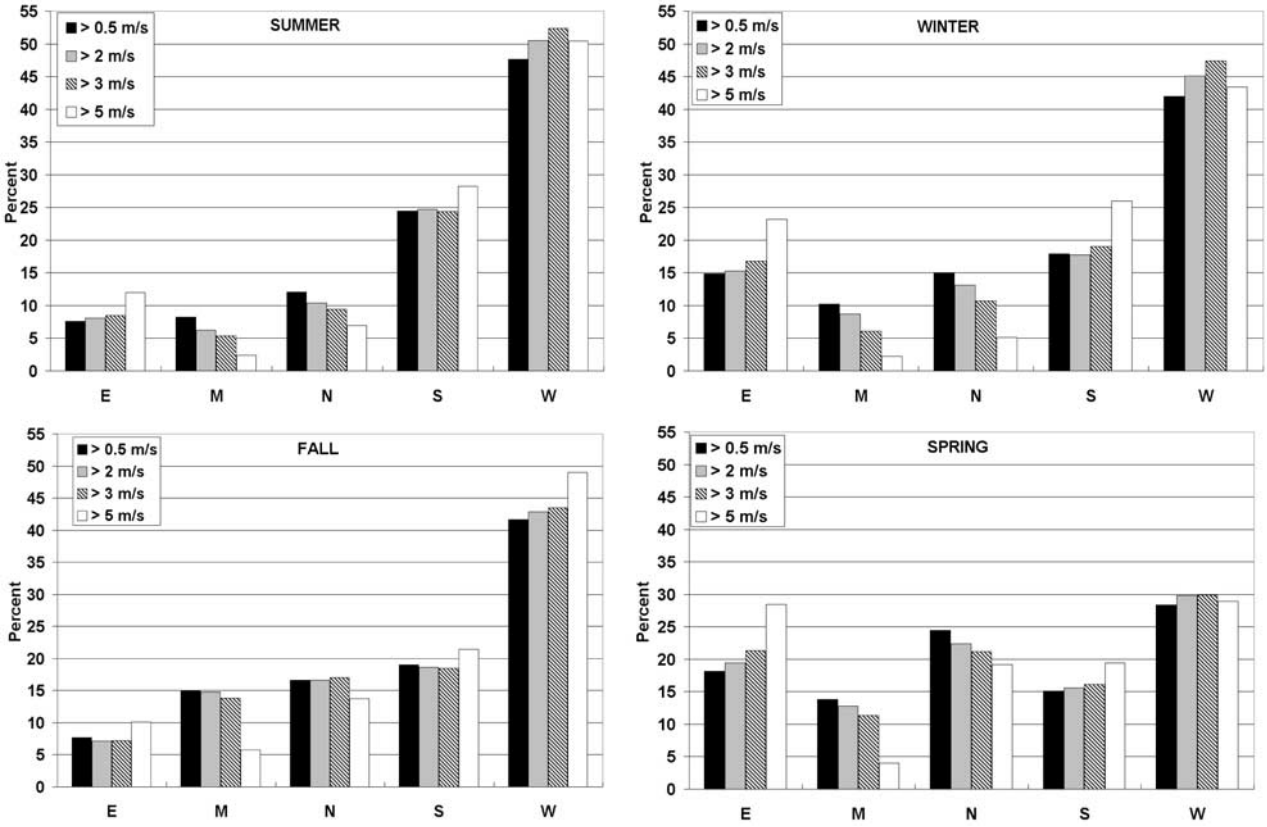

Figure 5. The percent occurrence of the hourly averaged locally measured wind direction in each sector for the summer, winter, fall and spring for minimum wind speed categories.

sectoring the data using the hourly local wind measurement. This comparison showed good agreement providing confidence that the measured wind direction is a good indicator to separate and identify source regions at the Sutton site. In addition, the local wind measurements were available every hour, whereas the trajectories were only available every 6 hours. The percent occurrence of the hourly-averaged locally measured wind direction in each sector using several minimum wind speed criteria is shown in Figure 5. The predominant wind direction was from the W sector for the summer, fall and winter with occurrences greater than 40%. In the summer, the next most common sector was S with almost 25% of the observations; less frequent were the M, N and E sectors, each less than 12%. For the spring, the highest number of observations also came from sector W (30%), but sectors N and E were not much less with ~22% and 20% of the observations respectively. In the following analysis, only sectors comprising air masses that passed over predominantly continental sources are considered (M, N, W and S); air masses in sector E were primarily marine-influenced, occurred infrequently and they are not further considered in this paper.

3.4. Partitioning of Reactive Nitrogen Oxide Species

[27] Figures 6 and 7 depict seasonal profiles for each air mass sector of the measured nitrogen oxide species and their contribution to NO_y. O_3, NO_y/O_3 and the ratio of the sum of the nitrogen oxide component species (denoted as NO_{yi}) to NO_y are also included. To improve the statistical robustness of Figures 6 and 7, the data have been grouped into two-month bins and each data point represents the median value. Only data is shown when the number of hours in a bin was greater than 15. The data for Figures 6 and 7 was generated from the hourly averaged database and included only measurements that were coincident in time (except NO_y because of the large data gap in the summer/fall 1998) and when the wind speed was greater than 2 m s^{-1} to minimize the impact of local emissions. The data in all the figures are only daytime measurements between 1000–1600 EST.

[28] Median NO_x levels decreased in most sectors from winter levels of approximately 1.5 ppbv to summer values near 0.5 ppbv. Emissions from Montreal were clearly influenced in air sampled from the northwest (sector M). In winter, the impact of Montreal emissions was not as distinct as in summer because of the increased NO_x levels in air from the other sectors. We believe that this is because the lifetime of NO_x in winter was long enough so that distances from source regions were less of a factor in determining the concentrations of NO_x at Sutton. From May–Aug, NO_x and NO_y mixing ratios were remarkably constant near 0.5 ppbv with little variability compared to the rest of the year. Substantial variability in NO_x levels was observed from Sep.–Apr., particularly in the M and N sectors compared to S and W sectors. It was expected that the N sector might represent background air masses, but the observed NO_x mixing ratios and NO_x/NO_y ratios in this sector were comparable to the other sectors for most months. Anthro-

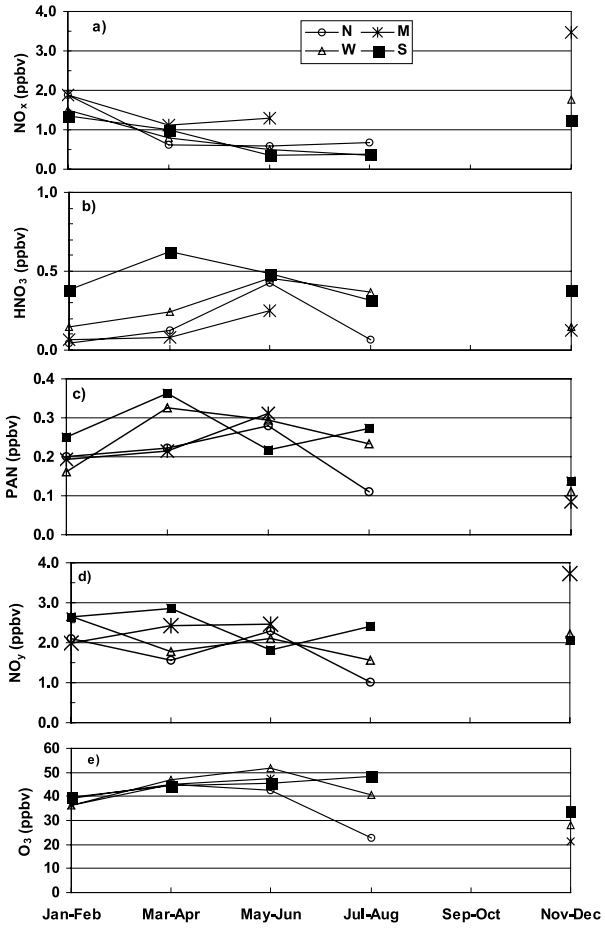

Figure 6. Seasonal profiles for each air mass sector of the measured nitrogen oxide species and O_3. The hourly data have been grouped into 2-month bins, and each data point represents the median value. The data are coincident daytime measurements between 1000 and 1600 EST.

pogenic sources of any significance in this sector would be the many small towns in the St. Lawrence River basin. In most cases, they are well within one day's travel and possibly account for the high NO_x/NO_y ratios in this sector (e.g., three main town centers ranging in population between 52,000 and 69,000 are within 90 km).

[29] HNO_3 levels were low in the winter months and increased through spring to maximize in May–June. The S sector exhibited an unusual increase to maximize in March–April that was distinct from the other sectors. Elevated summertime levels were observed in all sectors, but the M sector was markedly lower indicating that oxidation in air masses from this sector had not yet occurred to the same extent as sectors S, W and N. Lowest variability in HNO_3 levels was observed from November–February and increased in the other months. PAN mixing ratios in sectors S and W were on average higher than those in sectors M and N. The mixing ratios in sectors S and W peaked in the spring months (March–May), and in sectors N and M peaked in May–June. The lowest variability was observed in Nov–Dec with a marginal increase in variability from March to October The S and W sectors were generally higher in variability. *Bottenheim and Sirois* [1996] showed HNO_3 mixing ratios at Kejimkujik, Nova Scotia, Canada that exhibited similar seasonal variations as observed at Sutton, but their PAN data (over a 5 year period, 1984–1989) showed a more distinct springtime peak (March) in both polluted and background air masses.

[30] The seasonal partitioning of the individual nitrogen oxide species (see Figure 7) indicates that NO_x was the major component of NO_y during the winter months. On average, NO_x accounted for greater than 70% of the NO_y pool, while contributions from HNO_3 and PAN were less than 18% and 9% respectively. The NO_y reservoir in summer consisted of average contributions from NO_x, HNO_3 and PAN of 35%, 20–25% and 13% respectively. The NO_x/NO_y ratios exhibited a spring/summer decrease coincident with an increase in the HNO_3/NO_y and PAN/NO_y ratios reflecting enhanced conversion of NO_x to product species. As expected, the S and W sectors had the

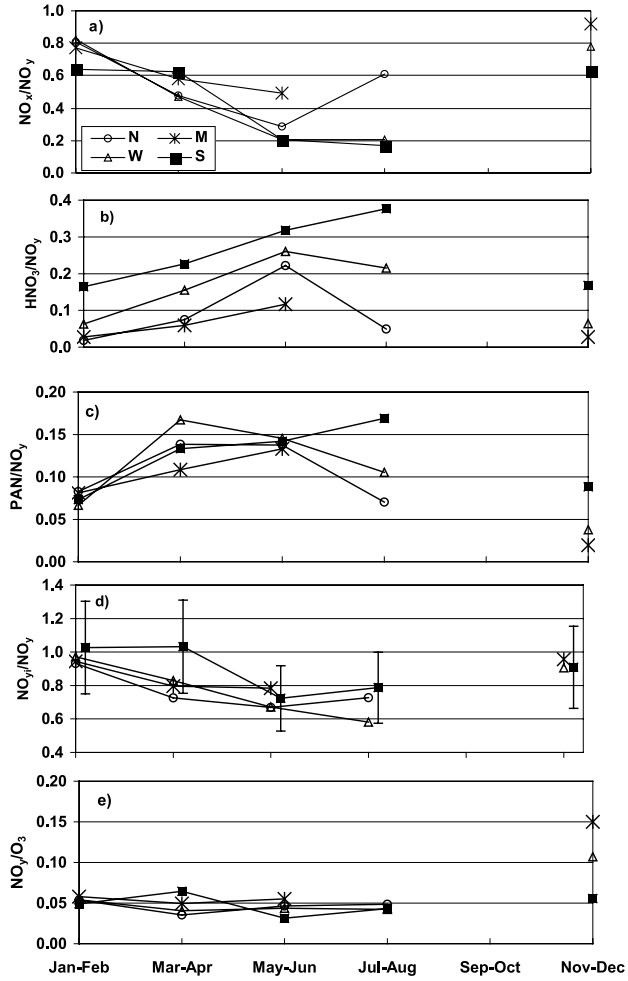

Figure 7. Seasonal profiles for each air mass sector of the median ratio of the component species and sum of component species (NO_{yi}) to NO_y, and NO_y/O_3. The hourly data have been grouped into 2-month bins and each data point represents the median value. The data are coincident daytime measurements between 1000 and 1600 EST.

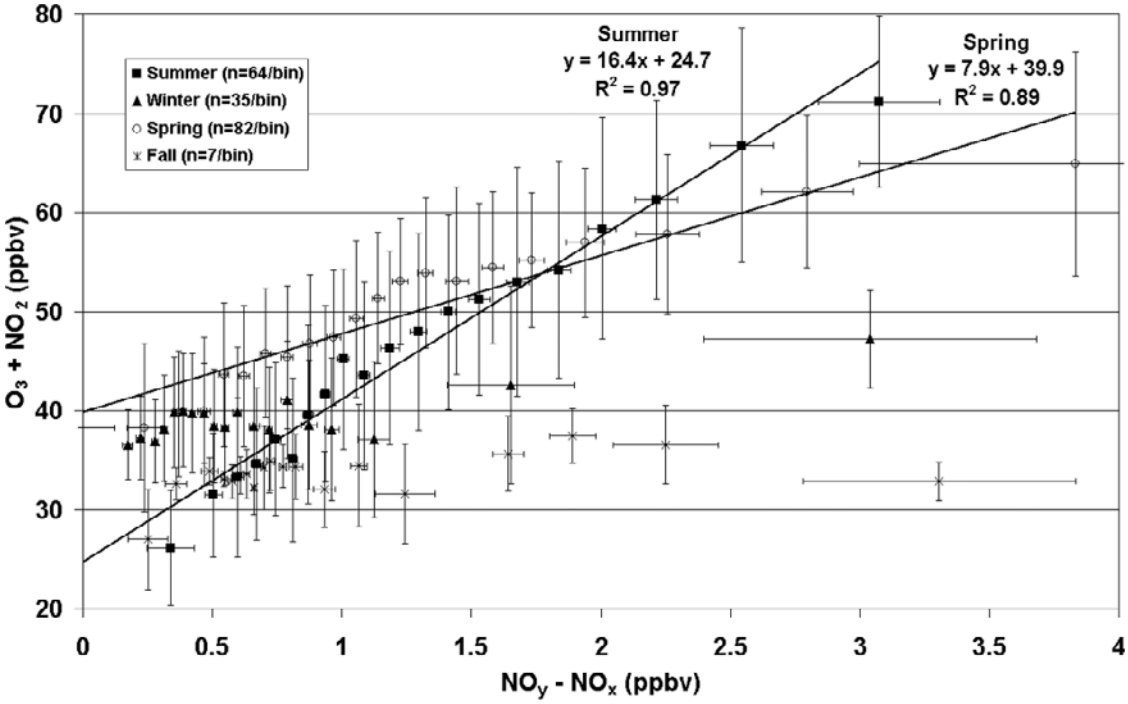

Figure 8. Correlation of odd oxygen versus $NO_y - NO_x$ (=NO_z) for each season during non-precipitating periods. Least squares linear fits to the averages of the hourly binned data and correlation coefficients are shown on the graph for summer and spring. The number of data points per bin are indicated in the legend. Each bin represents 5% of the data.

highest ratios (more so for HNO_3 than PAN) because of longer transit times from emission areas far upstream of Sutton. The persistence of high O_3 in the May–August period for these sectors is evidence of more extensive photochemical processing. In contrast, lower ratios of NO_x oxidation products to NO_y and lower O_3 in sectors N and M during summer are consistent with sources being quite close (discussed previously).

[31] In Figure 7d, the NO_{yi}/NO_y ratios indicates that the sum of NO_x, HNO_3 and PAN accounts for a large fraction of the measured NO_y, but, the extent of closure is seasonally dependent. In winter, greater than 90% of the NO_y was accounted for, but by spring and summer, there was an increase in the difference between the measured NO_y and NO_{yi} (i.e., NO_{yi}/NO_y decreased). This apparent NO_y deficit is discussed in more detail in section 3.6.3. At a receptor site like Sutton, the partitioning in any one sector is the result of the superposition of air mass histories related to emissions, meteorology, dilution and differential losses of species. Without detailed modeling it is difficult to assess the relative contribution from each of these factors to these ratios.

[32] The NO_y/O_3 ratios shown in Figure 7e range from 0.03 to 0.06 in units of ppbv $ppbv^{-1}$ (except November/December) and do not show a distinct dependence on air mass sector or season. *Ridley et al.* [1994] found that NO_y/O_3 ratios over the continental U.S. increased with decreasing altitude, maximizing at 0.03 ± 0.01 at the lowest measurement altitude of 2.4 km. By extrapolating this data to the Sutton altitude of about 1 km, the Sutton ratios are consistent with these aircraft measurements and are indicative of the planetary boundary layer rather than the more oxidized free troposphere (typical ratios 0.01 ± 0.04).

3.5. Ozone and $NO_y - NO_x$ Correlation

[33] A correlation of O_3 with ($NO_y - NO_x$) can provide an indication of the number of O_3 molecules produced, above a background O_3 level, per NO_x molecule oxidized. This ($NO_y - NO_x$) difference is also referred to in this paper as NO_z, and represents the oxidation products of NO_x. In rural areas, where NO_x mixing ratios are generally less than a few parts per billion, O_3 production is considered to be limited by the available NO_x and independent of the hydrocarbon concentrations [*Liu et al.*, 1987]. Uncertainties influencing this type of correlation using ambient measurements have been discussed by *Trainer et al.* [1993], the most significant being differences in removal rates of NO_y species and O_3. Despite these limitations, an examination of this relationship does provide useful insight into the sensitivity of O_3 production to NO_x oxidation. Figure 8 shows correlations of odd oxygen ($O_3 + NO_2$) (a more conserved quantity than O_3 alone) with the measured difference, ($NO_y - NO_x$) for each season. A high degree of correlation was found for both summer ($r^2 = 0.97$) and spring periods ($r^2 = 0.89$) for the entire range of ($NO_y - NO_x$) mixing ratios (<3–4 ppbv), indicating that O_3 production was highly sensitive to NO_x chemistry. The summertime slope of 16.4 at Sutton is somewhat higher than that for most rural sites, but not outside the range of reported values, 8–22 [*Hastie et al.*, 1996; *Olszyna et al.*, 1994; *Kleinman et al.*, 1994; *Hirsch et al.*, 1996; *Bottenheim and Sirois*, 1996; *Trainer et al.*, 1993; *Thornberry et al.*, 2001]. The differ-

ence between the summer (40 ppbv) and spring (25 ppbv) intercepts reflects the seasonal change in background, continental O_3 levels as measured at Sutton. This is substantiated by a comparison with O_3 measured in northerly (background) air masses at Mt. Tremblant (200 km north of Sutton, similar elevation) which showed spring and summer O_3 to be 40 and 28 ppbv respectively [*NO_x/VO_c Science Assessment*, 1997].

3.6. NO_y Deficit

[34] The presence of a NO_y deficit is not an unusual finding and has been widely reported in the literature [*Fahey et al.*, 1986; *Buhr et al.*, 1990; *Ridley et al.*, 1990; *Atlas et al.*, 1992; *Nielsen et al.*, 1995; *Aneja et al.*, 1996; *Williams et al.*, 1997; *Thornberry et al.*, 2001; *Volpe Horri*, 2002]. For example, at Harvard Forest, MA, under southwesterly flow (polluted), up to 50% of the NO_y was in excess of the sum of NO_x, HNO_3 and PAN [*Volpe Horri*, 2002]. In addition, at the PROPHET site in northern Michigan, *Thornberry et al.* [2001] compared the sum of the individual nitrogen oxides to the measured NO_y for ten 24-hr sampling periods (summer 1998) and reported the possibility of a NO_y shortfall of the order of 20%. In view of the observed NO_y deficit at Sutton, possible contributing factors will be discussed.

3.6.1. Measurement Uncertainties

[35] Considerable effort was undertaken to produce and confirm the quality of the measurements, including a detailed investigation into possible measurement problems that might have led to a NO_y deficit. Measurement uncertainties related to calibrations were minimized by cross checking the individual measurements, with the exception of HNO_3 and p-NO_3^-, against each other and against one common NIST-referenced standard. The comparison against one common standard reduces systematic calibration errors and absolute accuracies cancel in the ratios. The total propagated measurement uncertainties for each compound were as follows: NO_y (as NO) = 11%, NO_2 = 21%, NO = 16%, PAN = 20% and HNO_3 = 10%. On average, the total uncertainty of the sum of the individual components, NO_{yi}, was 17%, which is of course dependent upon the magnitude of the mixing ratios of the individual species. The resultant uncertainty in the NO_{yi}/NO_y ratios ranged from 25–30% for all seasons and all wind sectors. These are shown as error bars in Figure 7d; for clarity, only those for the S sector are shown. Despite this large uncertainty, the median values show a definite decrease from mid-winter to mid-summer.

[36] In Figure 9, mixing ratios and uncertainties of NO_y and NO_{yi} are compared for periods in December and May 1998 when all of the individual measurements were available. These months were selected as representative periods during the winter when the NO_y deficit was smallest to compare to the spring when the NO_y deficit was largest. During normal operation, daily 6-hour (1000–1600 EST) integrated HNO_3 mixing ratios were available, and thus the comparison was limited to one per day. In December, it can be seen that the sum of the individual measured component species, NO_{yi}, can account for the measured NO_y within the uncertainty of the measurements. These results are fairly typical during the winter months and indicate that on average there was no significant NO_y deficit during this period. However, the measurements in May indicate a number of days with a significant deficit in the sum of the individual measured species that falls outside the uncertainty of the measurements. The variability in the magnitude and/or presence of a NO_y deficit from day to day is also noted. This behaviour is characteristic of the spring and summer periods (see Figure 7d).

3.6.2. Measurement Interferences

[37] Interferences or processes were considered that could contribute to the NO_y signal or possibly reduce the signal in the separately measured NO_y species. Evaporated nitrate from particles collected on the Teflon filter at the front of the NO_y inlet system was considered as a possible suspect for NO_y signal enhancement. This type of interference was previously discussed in the context of the HNO_3/p-NO_3^- filter pack measurements. Net evaporation of NH_4NO_3 is most likely to occur under hot, dry conditions, and was not expected to be a significant problem for the measurement of NO_y at Sutton, particularly since aerosol loadings were generally quite low. In fact, data from the Intensive 1999 field study showed a significant NO_y deficit with average levels reaching 650 pptv (see Figure 10), and this period was characterized by frequent rain events and fairly cool temperatures. Furthermore, the inlet filters during this period were changed every day to minimize particle build-up. This particular two-week intensive sampling period seems to indicate that this is not a significant interference. Losses of HNO_3 on the NO_y inlet filter, which would indicate an even larger NO_y deficit, are also expected to be minimal because of low aerosol loadings at the Sutton site. During normal operation, the inlet filters were changed once per week by a local operator and an attempt was made to correlate the filter changes with differences in the NO_y signal/deficit. There was no evidence of a correlation, but admittedly, such a relationship would be difficult to establish under changing atmospheric conditions. Furthermore, even if evaporation or absorption of nitrate were significant interferences, the HNO_3 filter pack measurements would also be affected in the same manner and likely to the same magnitude, and, thus there would be no change to the NO_y deficit.

[38] Other potential interferences in the NO_y measurement include NH_3, HCN, and CH_3CN [*Kliner et al.*, 1997]. NH_3 was not measured during this field campaign, but during an earlier 1996 summer study at Sutton, NH_3 mixing ratios ranged from 0 to 3 ppbv, with average levels of 0.52 ± 0.53 ppbv with no consistent diurnal pattern (Anlauf, unpublished data), unlike the diurnal pattern found in the NO_y deficit discussed later (see Figure 10). *Williams et al.* [1998] evaluated several Mo converters and reported conversion efficiencies for NH3 in the range 0–8%. Using the average measured NH_3 at Sutton and a worst case conversion efficiency of 8%, an interference of 42 pptv could be expected. On the basis of these previous measurements, it is not expected to be a significant interference in the summer NO_y measurement. In the troposphere away from direct sources, HCN is typically 170 pptv and CH_3CN less than a few hundred pptv [*Hamm et al.*, 1989] and given the magnitude of NO_y mixing ratios at Sutton (low parts per billion), very little detectable interference from these species is expected. More rigorous testing of these molybdenum NO_y converters would be required to assess their conversion

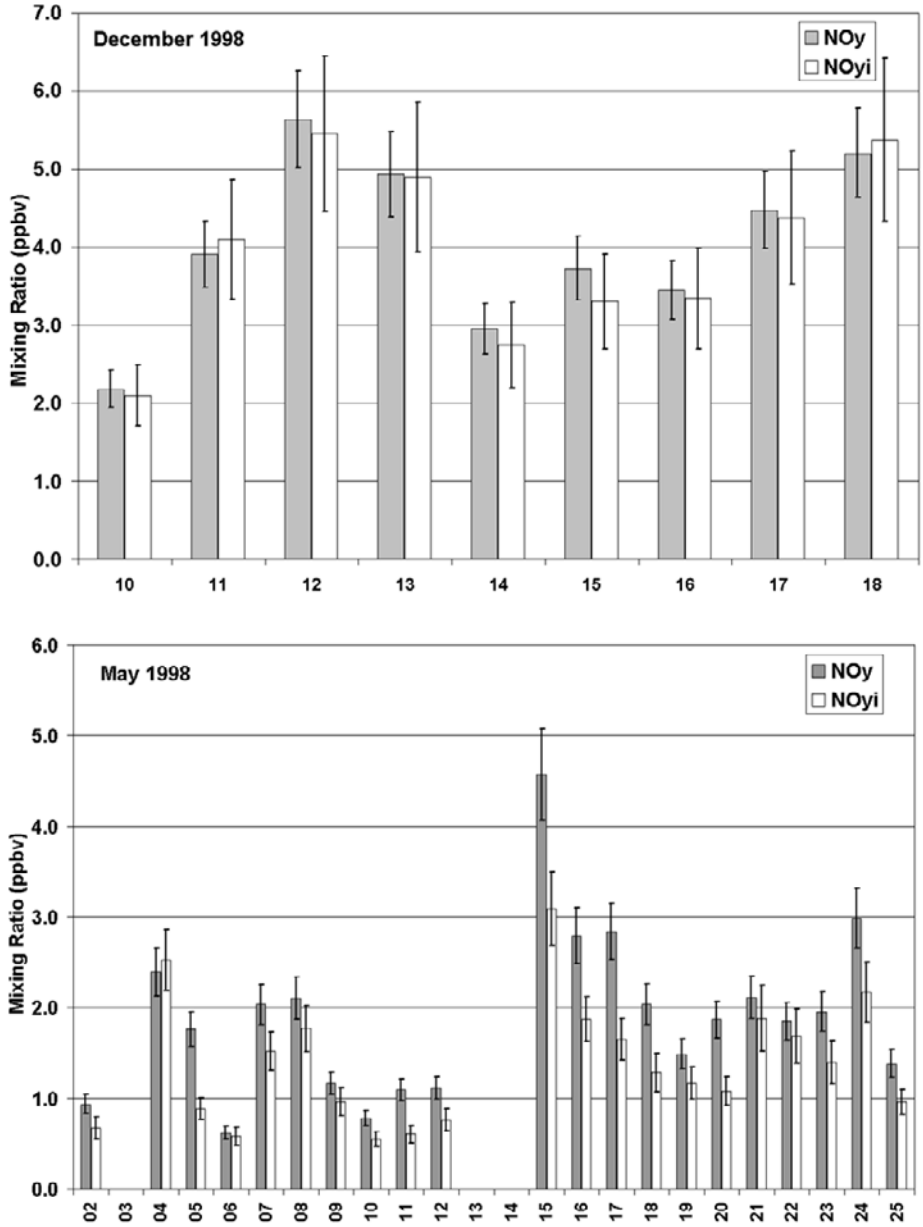

Figure 9. Mixing ratios of NO_y and NO_{yi} are compared for selected periods in December and May 1998 when all of the individual measurements are available. The error bars are the uncertainties in the measurements.

efficiencies of various nitrogen-containing compounds under various operating conditions such as converter temperature, humidity and ambient oxidant levels.

3.6.3. Unidentified Nitrogen Oxides in Ambient Air

[39] It has been speculated that the imbalance in the NO_y budget could be due to the presence of unidentified nitrogen oxide species in ambient air that contributed to the NO_y signal, but were not separately measured. Evidence suggests that organic nitrates, which are produced from the photochemical oxidation of hydrocarbons are possible candidates for these unidentified species [*Fahey et al.*, 1986; *Buhr et al.*, 1990]. Measurements of several of the smaller alkyl nitrates have indicated that they are generally a small fraction (less than a few percent) of the total NO_y [*Buhr et al.*, 1990; *Atlas et al.*, 1992; *Shepson et al.*, 1993; *Ostling et al.*, 2001], but it has been suggested that larger, multifunctional organic nitrates could be an important portion of the unidentified nitrogen species [*Shepson et al.*, 1993; *Grossenbacher et al.*, 2001]. This is consistent with speciated NO_y measurements made at the University of California Blodgett Forest Research Station using a thermal-dissociation-LIF (TD-LIF) technique; quantification of the sum total of alkyl nitrates and hydroxyalkyl nitrates showed that they can be as much as 25% of NO_y [*Day et al.*, 2000, 2002].

[40] The oxidation of biogenic hydrocarbons, particularly the isoprene + OH reaction, has been targeted as a potential pathway for significant formation of organic nitrates.

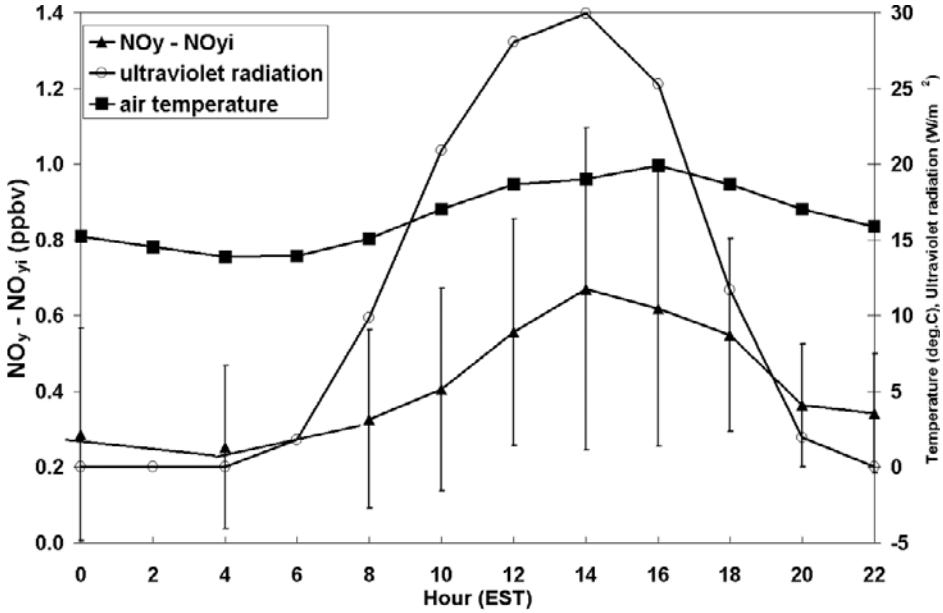

Figure 10. The diurnal variation of the unidentified NO_y (=NO_y − NO_{yi}), the ambient air temperature and ultraviolet radiation for the intensive 1999 period (June 27–July 15). Each data point represents the average value plotted at the end hour of a two-hour averaged sample. The error bars on the unidentified NO_y plot represent the standard deviation of the average value.

O'Brien et al. [1995] calculated that isoprene nitrates could possibly contribute to NO_y as much as the sum of all the organic nitrates (0.5–4%) that were quantitatively measured at a rural site in Ontario during the summer of 1992. In addition, recent measurements of isoprene nitrates at a forested site in Michigan ranged from 0.5–35 pptv and were 0.5–1.5% of NO_y, but up to 4% for well-aged air [*Grossenbacher et al.*, 2001].

[41] Since higher time-resolved HNO_3 measurements (2-hour) were available during a two-week period in the summer (June 27–July 15, 1999), it was possible to investigate the diurnal nature of the NO_y deficit. In Figure 10, the average unidentified NO_y (=NO_y − NO_{yi}) is plotted with the average ambient air temperature and ultraviolet radiation for this intensive measurement period as a function of time of day. The unidentified NO_y exhibited a similar profile to both the temperature and ultraviolet radiation. Average radiation levels maximized between 1200–1400 EST coincident with average values peaking near 0.67 ppbv of unidentified NO_y. A broad temperature maximum between 1000–1600 EST also corresponded to the largest average values of unidentified NO_y. The similar diurnal behaviour of the unidentified NO_y with ultraviolet radiation and air temperature suggests that the unidentified NO_y was photochemical in origin. A diurnal variation in the unidentified NO_y has also been noted by several other researchers [*Fahey et al.*, 1986; *Buhr et al.*, 1990; *Atlas et al.*, 1992]. *Buhr et al.* [1990] associated the diurnal behaviour of an unidentified fraction of NO_y at Scotia, PA in the summer of 1988 with that expected for organic nitrates, other than PAN. Its diurnal behaviour was remarkably similar to that observed at Sutton with maximum levels of the unidentified species close to 0.7 ppbv that occurred at 1400 EST. The fraction of unidentified NO_y at Sutton, however, ranged from 15–35% during the Intensive 1999 period, which was larger than that observed at Scotia (10–15%).

[42] Biogenic hydrocarbon emissions have been shown to play an important role in the summertime photochemistry at Sutton [*Macdonald et al.*, 2001]. In Figure 11, monthly averaged isoprene mixing ratios at Sutton are shown for 1998 and 1999 (Dann, private communication). Samples were collected in 3 L stainless steel Summa™ canisters integrated over 4-hours and analyzed by GC-FID. They show a distinct seasonal cycle with an onset of emissions in May, a maximum in June/July and a sharp drop off by mid-October. For the northern part of the Appalachian mountains in which the Sutton site is located, the development of leaves on the trees does not occur until well into the spring period (mid-May). As a result, isoprene emissions would be negligible in early spring. However, by June and July, there is full leaf foliage and temperatures and radiation are conducive to maximum isoprene emissions. Emissions of monoterpenes are primarily controlled by temperature [*Guenther*, 1997] and are expected to exhibit a similar seasonal profile to that of isoprene. Figure 11 also shows the average monthly unidentified NO_y for 1998 and 1999. Although a significant portion of the NO_y was unaccounted for during the summer months and corresponded to elevated isoprene levels, the unidentified NO_y spring maximum was much earlier than that of isoprene. Thus although the oxidation of isoprene could contribute to the observed summertime unidentified NO_y, it cannot explain the early springtime maximum. Hence it is difficult to understand why the unidentified NO_y maximized in the springtime.

[43] To further characterize the seasonal NO_y deficit, correlations of the unidentified NO_y with 1 − NO_x/NO_y, a surrogate for photochemical age, are shown in Figure 12

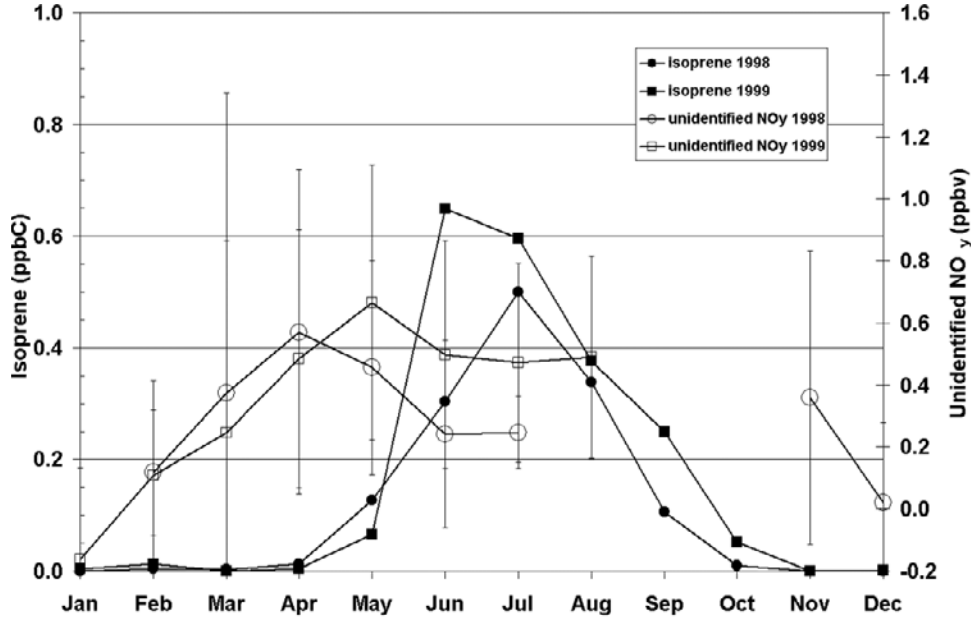

Figure 11. Average mixing ratios the unidentified NO_y and isoprene for 1998 and 1999 as a function of month. The error bars represent the standard deviation of the average value.

for the winter, spring and summer seasons. In all seasons, the average unidentified NO_y was fairly constant at about 250 pptv below a photochemical age of 0.7, but these values are considered to be close to or within the error of the measurements. In the spring and summer, the unidentified NO_y exhibited strong correlations with photochemical ages greater than 0.7. The distinct increase in the $NO_y - NO_{yi}$ difference at photochemical ages greater than 0.7 indicates that the presence of the unidentified NO_y species is most notable in highly processed air mass conditions. The NO_y deficit also correlates with O_3, temperature and solar radiation probably because, in turn, these are associated with highly processed air masses. All source sectors exhibited an increase in unidentified NO_y

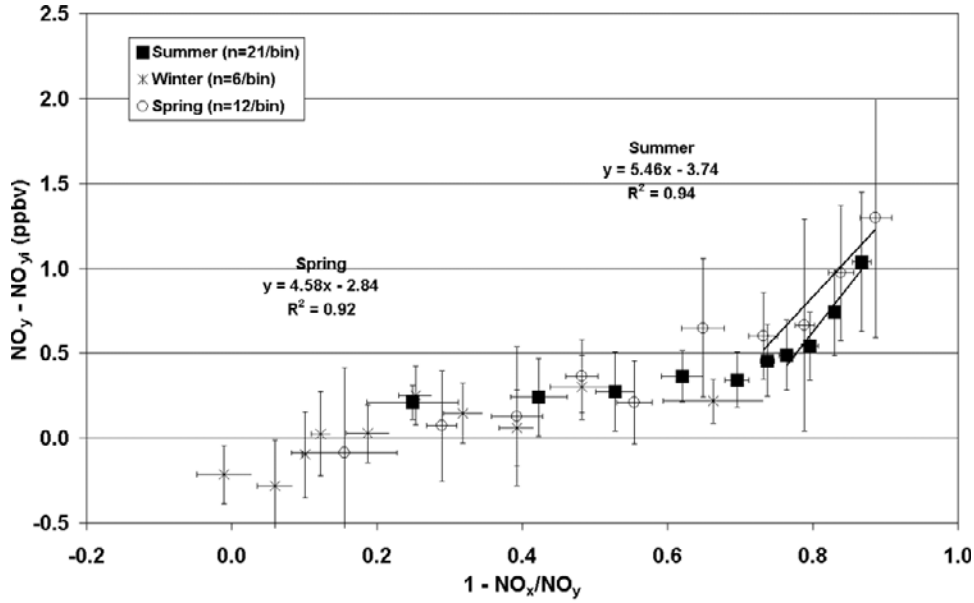

Figure 12. Correlations of the unidentified NO_y (=$NO_y - NO_{yi}$) with $1 - NO_x/NO_y$ for the winter, spring and summer. The data that were averaged over the HNO_3 sampling interval were sorted by the abscissa and divided into bins where each bin represents 10% of the data. Averages and standard deviations (vertical and horizontal bars) were calculated for the appropriate variables in each bin. Results of linear least squares fits to the averages of each bin are shown on the figures. The abscissa, $1 - NO_x/NO_y$, represents the degree of photochemical processing.

(where $1 - NO_x/NO_y > 0.7$) for both the summer and spring, but it was largest in magnitude and most frequent from the S and W sectors.

4. Conclusions

[44] Measurements of the major reactive nitrogen oxides including NO, NO_2, HNO_3, particulate nitrate, PAN and NO_y, as well as O_3 and supporting meteorology, were made at a high-elevation site (845 masl) in the rural eastern townships of Quebec, Canada from February 1998 to August 1999. NO_x (and NO_y) mixing ratios exhibited a distinct seasonal cycle with median NO_x levels in winter more than a factor of 4 greater than in summer. Since the source strength of NO_x and daytime boundary layer heights do not appear to be seasonally dependent, photochemistry must play a dominant role in determining seasonal nitrogen oxide levels. These results are consistent with those from another rural site in northeastern North America [*Munger et al.*, 1996, 1998].

[45] The seasonal partitioning of the individual nitrogen oxide species indicates that NO_x was the major component of NO_y during the winter months. On average, NO_x accounted for greater than 70% of the NO_y pool, while contributions from HNO_3 and PAN were less than 18% and 9% respectively. The NO_y reservoir in summer consisted of average contributions from NO_x, HNO_3 and PAN of 35%, 20–25% and 13% respectively. The NO_x/NO_y ratios exhibited a spring/summer decrease coincident with an increase in the HNO_3/NO_y and PAN/NO_y ratios reflecting enhanced conversion of NO_x to product species. The S and W sectors had the highest ratios because of longer transit times, and thus more extensive photochemical processing, from emission areas far upstream of Sutton. The sum of NO_x, HNO_3 and PAN accounted for a large fraction of the measured NO_y, but the extent of closure was seasonally dependent. In winter, greater than 90% of the NO_y was accounted for, but by spring and summer, there was an increase in the difference between the measured NO_y and NO_{yi} (i.e., NO_{yi}/NO_y decreased) of the order of 25–30%. This NO_y deficit could not be explained by measurement uncertainties or potential interferences. It is possible that there were other reactive nitrogen species in the atmosphere that were not separately measured that contributed to the NO_y deficit. Indications are that these compounds were photochemically produced and present in highly processed air masses. The key to their identification, in part, may be in the complete understanding of seasonal biogenic variations in emissions and their oxidation mechanisms, particularly in relation to organic nitrates.

[46] **Acknowledgments.** The authors would like to thank Maurice Watt, Nicolas Durand, Catherine Frizzle, and Mark Mailloux for their technical assistance. We would also like to thank the reviewers of this paper for their helpful suggestions and comments.

References

Aneja, V. P., C. S. Claiborn, Z. Li, and A. Murthy, Trends, seasonal variations, and analysis of high-elevation surface nitric acid, ozone, and hydrogen peroxide, *Atmos. Environ.*, *28*, 1781–1790, 1994.

Aneja, V. P., D.-S. Kim, M. Das, and B. E. Hartsell, Measurements and analysis of reactive nitrogen species in the rural troposphere of southeast United States: Southern Oxidant Study site Sonia, *Atmos. Envrion.*, *30*, 649–659, 1996.

Anlauf, K. G., H. A. Wiebe, and P. Fellin, Characterization of several integrative sampling methods for nitric acid, sulphur dioxide and atmospheric particles, *JAPCA*, *36*, 715–723, 1986.

Anlauf, K. G., D. MacTavish, H. A. Wiebe, and G. Mackay, Measurement of atmospheric nitric acid and ammonia by the filter method and a comparison to the tuneable diode laser method, in *Proceedings of the 1987 EPA/APCA Symposium on Measurement of Toxic and Related Air Pollutants*, *EPA Rep. 600/9-87-010*, pp. 373–378, APCA, Pittsburgh, Pa., 1987.

Atlas, E. L., B. A. Ridley, G. Hübler, J. G. Walega, M. A. Carroll, D. D. Montzka, B. J. Huebert, R. B. Norton, F. E. Grahek, and S. Schauffler, Partitioning and budget of NO_y species during the Mauna Loa Observatory Photochemical Experiments, *J. Geophys. Res.*, *97*, 10,449–10,462, 1992.

Bollinger, M. J., Chemiluminescent measurements of the oxides of nitrogen in the clean troposphere and atmospheric chemistry implications, Ph.D. thesis, Univ. of Colo., Boulder, Colo., 1982.

Bottenheim, J. W., and A. Sirois, Long-term daily mean mixing ratios of O_3, PAN, HNO_3, and particle nitrate at a rural location in eastern Canada: Relationships and implied ozone production efficiency, *J. Geophys. Res.*, *101*, 4189–4204, 1996.

Buhr, M. P., D. D. Parrish, R. B. Norton, F. C. Fehsenfeld, and R. E. Sievers, Contribution of organic nitrates to the total reactive nitrogen budget at a rural eastern U. S. site, *J. Geophys. Res*, *95*, 9809–9816, 1990.

Carroll, M. A., and A. M. Thompson, NO_x in the non-urban troposphere, in *Progress and Problems in Atmospheric Chemistry*, ch. 7, pp. 198–255, 1995.

Day, D. A., P. J. Wooldridge, M. B. Dillon, and R. C. Cohen, Observations of HNO_3, alkyl nitrates, and peroxynitrates in the Sacramento plume, *Eos Trans. AGU*, *81*(48), Abstract A21E-09, 2000.

Day, D. A., P. J. Wooldridge, M. B. Dillon, J. A. Thornton, and R. C. Cohen, A thermal dissociation laser-induced fluorescence instrument for in situ detection of NO_2, peroxy nitrates, alkyl nitrates, and HNO_3, *J. Geophys. Res.*, *107*(D6), 4046, doi:10.1029/JD/2001/000779, 2002.

Emmons, L. K., et al., Climatologies of NO_x and NO_y: A comparison of data and models, *Atmos. Eviron.*, *31*, 1851–1904, 1997.

Fahey, D. W., G. Hübler, D. D. Parrish, E. J. Williams, R. B. Norton, B. A. Ridley, H. B. Singh, S. C. Liu, and F. C. Fehsenfeld, Reactive nitrogen species in the troposphere: Measurements of NO, NO_2, HNO_3, particulate nitrate, peroxyacetyl nitrate (PAN), O_3, and total reactive odd nitrogen (NO_y) at Niwot Ridge, Colorado, *J. Geophys. Res.*, *91*, 9781–9793, 1986.

Fehsenfeld, F. C., et al., Intercomparison of NO_2 measurement techniques, *J. Geophys. Res.*, *95*, 3579–3597, 1990.

Fehsenfeld, F. C., L. G. Huey, D. T. Sueper, R. B. Norton, E. J. Williams, F. L. Eisele, R. L. Mauldin III, and D. J. Tanner, Ground-based intercomparison of nitric acid measurement techniques, *J. Geophys. Res.*, *103*, 3343–3353, 1998.

Forrest, J., D. J. Spandau, R. L. Tanner, and L. Newman, Determination of atmospheric nitrate and nitric acid employing a diffusion denuder with a filter pack, *Atmos. Environ.*, *16*, 1473–1485, 1982.

Grossenbacher, J. W., et al., Measurements of isoprene nitrates above a forest canopy, *J. Geophys. Res.*, *106*, 24,429–24,438, 2001.

Guenther, A., Seasonal and spatial variations in natural volatile organic compound emissions, *Ecol. Appl.*, *7*, 34–45, 1997.

Hamm, S., G. Helas, and P. Warneck, Acetonitrile in the air over Europe, *Geophys. Res. Lett.*, *16*, 483–486, 1989.

Hastie, D. R., P. B. Shepson, N. Reid, P. B. Roussel, and O. T. Melo, Summertime NO_x, NO_y, and Ozone at a site in rural Ontario, *Atmos. Environ.*, *103*, 2157–2165, 1996.

Hirsch, A. I., J. W. Munger, D. J. Jacob, L. W. Horowitz, and A. H. Goldstein, Seasonal variation of the ozone production efficiency per unit NO_x at Harvard Forest, Massachusetts, *J. Geophys. Res.*, *101*, 12,659–12,666, 1996.

Holzworth, G. C., Mixing depths, wind speeds and air pollution potential for selected locations in the United States, *J. Appl. Meteorol.*, *6*, 1039–1044, 1967.

Kleinman, L., et al., Ozone formation at a rural site in the southeastern United States, *J. Geophys. Res.*, *99*, 3469–3482, 1994.

Kliner, D. A. V., B. C. Daube, J. D. Burley, and S. C. Wofsy, Laboratory investigation of the catalytic reduction technique for measurement of atmospheric NO_y, *J. Geophys. Res.*, *102*, 10,579–10,776, 1997.

Liu, S. C., M. Trainer, F. C. Fehsenfeld, D. D. Parrish, E. J. Williams, D. W. Fahey, G. Hüber, and P. C. Murphy, Ozone production in the rural troposphere and the implications of regional and global ozone distribution, *J. Geophys. Res.*, *94*, 4191–4207, 1987.

Macdonald, A. M., P. A. Makar, K. G. Anlauf, K. L. Hayden, J. W. Bottenheim, D. Wang, and T. Dann, Summertime formaldehyde at a high-elevation site in Quebec, *J. Geophys. Res*, *106*, 32,361–32,374, 2001.

Meteorological Service of Canada, Precursor contributions to ambient fine particulate matter in Canada, Atmos. And Clim. Sci. Dir., Meteorol. Serv. of Can., Downsview, Ontario, Canada, 2001.

Munger, J. W., S. C. Wofsy, P. S. Bakwin, S. Fan, M. L. Goulden, B. C. Daube, and A. H. Goldstein, Atmospheric deposition of reactive nitrogen oxides and ozone in a temperate deciduous forest and a subarctic woodland: 1. Measurements and mechanisms, *J. Geophys. Res.*, *101*, 12,639–12,657, 1996.

Munger, J. W., S. M. Fan, P. S. Bakwin, M. L. Goulden, A. H. Goldstein, A. S. Colman, and S. C. Wofsy, Regional budgets for nitrogen oxides from continental sources: Variations of rates of oxidation and deposition with season and distance from source regions, *J. Geophys. Res.*, *103*, 8355–8368, 1998.

Neilsen, T., A. H. Egelov, K. Granby, and H. Skov, Observations on particulate organic nitrates and unidentified components of NO_y, *Atmos. Environ.*, *29*, 1757–1769, 1995.

NO_x/VO_c Science Assessment, Ground-level ozone and its precursors, 1980–1993, *Rep. of the Data Anal. Working Group, Sect. 2.1.2*, *Cat. En56-167/2001E*, Publ. Works and Gov. Serv., Ontario, Canada, 1997.

O'Brien, J. M., P. B. Shepson, K. Muthuramu, C. Hao, H. Niki, and D. R. Hastie, Measurements of alkyl and multifunctional organic nitrates at a rural site in Ontario, *J. Geophys. Res.*, *100*, 22,795–22,804, 1995.

Olson, M. P., K. K. Oikawa, and A. W. MacAfee, A trajectory model applied to LRTAP: A technical description and some model intercomparisons, *Rep. LRTAP 78-4*, *Atmos. Environ. Ser.*, Air Qual. Res. Branch, Ontario, Canada, 1978.

Olszyna, K. J., E. M. Bailey, R. Simonaitis, and J. F. Meagher, O_3 and NO_y relationships at a rural site, *J. Geophys. Res.*, *99*, 14,557–14,563, 1994.

Ostling, K., B. Kelly, S. Bird, S. Bertman, and M. Pippin, Fast-turnaround alkyl nitrate measurements during the PROPHET 1998 summer intensive, *J. Geophys. Res.*, *106*, 24,439–24,449, 2001.

Parrish, D. D., et al., The total reactive oxidized nitrogen levels and the partitioning between the individual species at six rural sites in eastern North America, *J. Geophys. Res.*, *98*, 2927–2939, 1993.

Pätz, H. W., A. Lerner, N. Houben, and A. Volz-Thomas, Validierung eines neuen Verfahrens zur Kalibrierung von Peroxiacetylnitrat (PAN), *Anal. Gefahrstoffe Reinhaltung Luft*, *62*, 215–219, 2002.

Ridley, B. A., M. A. Carroll, G. L. Gregory, and G. W. Sachse, NO and NO_2 in the troposphere: Technique and measurements in regions of a folded tropopause, *J. Geophys. Res.*, *93*, 15,813–15,830, 1988.

Ridley, B. A., J. D. Shetter, J. G. Walega, S. Madronich, C. M. Elsworth, and F. E. Grahek, The behavior of some organic nitrates at Boulder and Niwot Ride, Colorado, *J. Geophys. Res.*, *95*, 13,949–13,961, 1990.

Ridley, B. A., J. G. Walega, J. E. Dye, and F. E. Grahek, Distributions of NO, NO_x, NO_y, and O_3 to 12 km altitude during the summer monsoon season over New Mexico, *J. Geophys. Res.*, *99*, 25,519–25,534, 1994.

SENES Consultants Ltd., A mixing height study for North America (1987–1991), Meteorol. Serv. of Can., Toronto, Ontario, Canada, 1997.

Shepson, P. B., K. G. Anlauf, J. W. Bottenheim, H. A. Wiebe, N. Gao, K. Muthuramu, and G. I. Mackay, Alkyl nitrates and their contribution to reactive nitrogen at a rural site in Ontario, *Atmos. Environ., Part A*, *27*, 749–757, 1993.

Spicer, C. W., J. E. Howes Jr., T. A. Bishop, L. H. Arnold, and R. K. Stevens, Nitric acid measurement methods: An intercomparison, *Atmos. Environ.*, *16*, 1487–1500, 1982.

Thornberry, T., et al., Observations of reactive oxidized nitrogen and speciation of NO_y during the PROPHET summer 1998 intensive, *J. Geophys. Res.*, *106*, 24,359–24,386, 2001.

Trainer, M., E. Y. Hsie, S. A. McKeen, R. Tallamraju, D. D. Parrish, F. C. Fehsenfeld, and S. C. Liu, Impact of natural hydrdocarbons on hydroxyl and peroxy radicals at a remote site, *J. Geophys. Res.*, *92*, 11,879–11,894, 1987.

Trainer, M., et al., Correlation of ozone with NO_y in photochemically aged air, *J. Geophys. Res.*, *98*, 2917–2925, 1993.

Volpe Horri, C., Tropospheric reactive nitrogen speciation, deposition, and chemistry at Harvard Forest, Ph.D. thesis, Harvard Univ., Boston, Mass., April 2002.

Williams, E. J., J. M. Roberts, K. Baumann, S. B. Bertman, S. Buhr, R. B. Norton, and F. C. Fehsenfeld, Variations in NO_y composition at Idaho Hill, Colorado, *J. Geophys. Res.*, *102*, 6297–6314, 1997.

Williams, E. J., et al., Intercomparison of ground-based NO_y measurement techniques, *J. Geophys. Res.*, *103*, 21,261–22,280, 1998.

K. G. Anlauf, J. W. Bottenheim, and K. L. Hayden, Meteorological Service of Canada, Environment Canada, 4905 Dufferin Street, Toronto, Ontario, Canada M3H 5T4. (katharine.hayden@ec.gc.ca)

D. R. Hastie, York University, 4700 Keele Street, Toronto, Ontario, Canada M3J 1P3.